

Semiclassical calculation of collisional dissociation cross sections for $N+N_2$

Catherine Tully^{a)} and Robert E. Johnson

Department of Engineering Physics and Astronomy, Thornton Hall, University of Virginia, Charlottesville, Virginia 22903

(Received 5 April 2002; accepted 11 July 2002)

Dissociation and doubly differential cross sections are calculated for $N+N_2$ at near-threshold collision energies using a semiclassical wave packet method in which the vibrational motion of the molecule is treated quantum mechanically and the rotational and translational motions are treated classically. A three-bodied London–Eyring–Polanyi–Sato potential energy surface is used and results compared to those obtained using a purely repulsive power law potential. For a comparison of results, cross sections are also calculated using pure classical mechanics. © 2002 American Institute of Physics. [DOI: 10.1063/1.1504085]

I. INTRODUCTION

The collision-induced dissociation (CID) of the N_2 molecule by an energetic nitrogen atom is a process of importance in the upper atmosphere of Titan, a moon of Saturn, which has a nitrogen atmosphere.¹ The energized nitrogen atoms produced by dissociation populate Titan's atmospheric corona and can contribute to atmospheric loss. Essentially no laboratory data exist for this collisional system in the energy range of interest (~ 9 eV to \sim a few keV). Previously Johnson *et al.*² calculated the collisional dissociation cross sections for $N+N_2$ using classical molecular dynamics and potentials constructed based on laboratory data for energy transfer in $O+N_2$ collisions.³ They found that for a number of atom–molecule collisions the classical dissociation threshold using repulsive power law potentials is about three times the actual dissociation energy. They also concluded that classical trajectory calculations were reasonably accurate at high energies but poorly describe the effective threshold. Since dissociation can occur down to the true threshold it is important to carry out a more detailed calculation in this regime.

A full quantum mechanical calculation for CID is computationally challenging, particularly when such a large number of rotational channels participate in the collision. Quantum mechanical effects become most significant when tunneling occurs or when the energy spacings between the quantum states are large. In investigating the system $N+N_2 \rightarrow N+N+N$, since tunneling plays no role and the rotational levels of the N_2 molecule are closely spaced, we have employed a semiclassical approximation. The vibrational motion of the N_2 molecule is treated quantum mechanically, using a time-dependent wave packet method, while the rotational motions and the relative translational motion are treated classically. This approach has previously been applied to atom–diatom reactive systems⁴ and to more complex

molecule–molecule reactive⁵ and nonreactive⁶ scattering problems.

This paper is organized as follows: The theory behind the calculation is given in Sec. II, where we introduce the semiclassical effective Hamiltonian (Sec. II A) and describe the method of solution (Sec. II B), including the wave packet propagation techniques. We also briefly review the equations for calculating the dissociation cross sections in Sec. II C. In Sec. III the computational details of the calculation are given along with the results for the total integrated dissociation cross sections and the doubly differential cross sections. A summary of our findings is given in Sec. IV.

II. THEORY AND CALCULATION

A. Semiclassical equation

To study the system $A+BC \rightarrow A+B+C$ we use the space fixed Jacobi coordinate system where \mathbf{r}_1 is the vector joining atom B to C and \mathbf{r}_2 is the vector joining atom A to the center of mass of molecule BC. The Hamiltonian for this system is given by

$$\hat{H} = - \sum_{i=1}^2 \frac{\hbar^2}{2\mu_i} \left[\frac{\partial^2}{\partial r_i^2} + \frac{2}{r_i} \frac{\partial}{\partial r_i} + \frac{1}{r_i^2} \left(\frac{\partial^2}{\partial \theta_i^2} + \cot \theta_i \frac{\partial}{\partial \theta_i} + \frac{1}{\sin^2 \theta_i} \frac{\partial^2}{\partial \phi_i^2} \right) \right] + V(r_i, \theta_i, \phi_i), \quad i=1,2, \quad (1)$$

where the vector \mathbf{r}_i is expressed in terms of spherical polar coordinates r_i , θ_i , and ϕ_i . θ_i and ϕ_i are the angles defining the orientation of the space fixed vectors \mathbf{r}_i . μ_1 is the reduced mass of the molecule BC and μ_2 is the three-body reduced mass. If Ψ is the wave function associated with the Hamiltonian of Eq. (1), we can introduce a new wave function ψ , given by

$$\psi = r_1 \Psi, \quad (2)$$

so that the first derivative in r_1 in Eq. (1) is eliminated. The semiclassical Hamiltonian is then obtained by replacing the

^{a)}Present address: Department of Chemistry, H. C. Ørsted Institute, University of Copenhagen, DK-2100 Ø Copenhagen, Denmark. Electronic mail: catherine@theory.ki.ku.dk

variables associated with the translational and rotational motions in Eq. (4) with their respective classical counterparts, i.e.,

$$\hat{H}_{sc} = \frac{-\hbar^2}{2\mu_1} \frac{\partial^2}{\partial r_1^2} + \frac{P_{r_2}^2}{2\mu_2} + \sum_{i=1}^2 \frac{1}{2\mu_i r_i^2} \left(P_{\theta_i}^2 + \frac{1}{\sin^2 \theta_i} P_{\phi_i}^2 \right) + V(r_i, \theta_i, \phi_i), \quad i=1,2. \quad (3)$$

In Eq. (3), the \mathbf{P}_i are the classical momentum associated with r_2 and the orientation angles. The effective semiclassical Hamiltonian, which is defined as the expectation value of the semiclassical Hamiltonian, couples the classical and semiclassical degrees of freedom. It is given by

$$\begin{aligned} \hat{H}_{sc}^{\text{eff}} &= \frac{\langle \psi | \hat{H}_{sc} | \psi \rangle}{\langle \psi | \psi \rangle} \\ &= \hat{H}_Q^{\text{eff}} + \frac{P_{r_2}^2}{2\mu_2} + \frac{1}{2\mu_2 r_2^2} \left(P_{\theta_2}^2 + \frac{1}{\sin^2 \theta_2} P_{\phi_2}^2 \right) \\ &\quad + \frac{1}{2\mu_1} \left(P_{\theta_1}^2 + \frac{1}{\sin^2 \theta_1} P_{\phi_1}^2 \right) \left(\frac{1}{r_1^2} \right)^{\text{eff}} \\ &\quad + V^{\text{eff}}(r_i, \theta_i, \phi_i), \quad i=1,2, \end{aligned} \quad (4)$$

where

$$\hat{H}_Q^{\text{eff}} = \frac{\langle \psi | \hat{H}_Q | \psi \rangle}{\langle \psi | \psi \rangle}, \quad (5)$$

$$\hat{H}_Q = \frac{-\hbar^2}{2\mu_1} \frac{\partial^2}{\partial r_1^2}, \quad (6)$$

$$\left(\frac{1}{r_1^2} \right)^{\text{eff}} = \frac{\langle \psi | \frac{1}{r_1^2} | \psi \rangle}{\langle \psi | \psi \rangle}, \quad (7)$$

and

$$V^{\text{eff}}(r_i, \theta_i, \phi_i) = \frac{\langle \psi | V(r_i, \theta_i, \phi_i) | \psi \rangle}{\langle \psi | \psi \rangle}. \quad (8)$$

In the above equations $\langle \rangle$ denotes integration over the quantal variable r_1 .

B. Method of solution

For the quantal part of the calculation the time-dependent Schrödinger equation is given by

$$i\hbar \frac{\partial \psi(r_1, t)}{\partial t} = \left[\frac{-\hbar^2}{2\mu_1} \frac{\partial^2}{\partial r_1^2} + \frac{1}{2\mu_1 r_1^2} \left(P_{\theta_1}^2 + \frac{1}{\sin^2 \theta_1} P_{\phi_1}^2 \right) + V(r_i, \theta_i, \phi_i) \right] \psi(r_1, t). \quad (9)$$

During the propagation of the wave function, the variables r_2 , θ_i , and ϕ_i , $i=1,2$ and the momenta, $P_{\theta_1}^2$ and P_{ϕ_1} , were passed from the classical calculation and remained constant for each time step Δt . The wave packet propagation was carried out using the symmetrized split operator (SSO) fast Fourier transform (FFT) method⁷ and a finite grid, which is described briefly in the Appendix. The initial wave function

$\psi(r_1, t=0)$ in the vibrational state v was taken as a Morse oscillator wave function. Because we will use the population of the bound states below, we eliminate the reactive and dissociative contributions to the wave function by introducing an absorbing potential,

$$V_{\text{abs}} = \begin{cases} -iV_0 \Delta t (r_1 - r_{\text{abs}}) / \hbar \Delta r_{\text{abs}}, & r_{\text{abs}} < r_1 \leq r_{\text{abs}} + \Delta r_{\text{abs}} \\ 0, & r_1 \leq r_{\text{abs}}, \end{cases} \quad (10)$$

where V_0 is the height and Δr_{abs} the width of the absorbing potential and r_{abs} is its location on r_1 , which is placed sufficiently far away from the interaction region. This procedure also prevents any reflection at the boundaries that arise naturally in the SSO FFT method.⁸

The classical equations of motion, given by

$$\begin{aligned} \dot{\theta}_1 &= \frac{P_{\theta_1}}{\mu_1} \left(\frac{1}{r_1^2} \right)^{\text{eff}}, \\ \dot{P}_{\theta_1} &= \frac{P_{\phi_1}^2 \cos \theta_1}{\mu_1 \sin^3 \theta_1} \left(\frac{1}{r_1^2} \right)^{\text{eff}} - \frac{\partial V^{\text{eff}}(r_i, \theta_i, \phi_i)}{\partial \theta_1}, \\ \dot{\phi}_1 &= \frac{P_{\phi_1}}{\mu_1 \sin^2 \theta_1} \left(\frac{1}{r_1^2} \right)^{\text{eff}}, \quad \dot{P}_{\phi_1} = -\frac{\partial V^{\text{eff}}(r_i, \theta_i, \phi_i)}{\partial \phi_1}, \\ \dot{r}_2 &= \frac{P_{r_2}}{\mu_2}, \\ \dot{P}_{r_2} &= \left(P_{\theta_2}^2 + \frac{P_{\phi_2}^2}{\sin^2 \theta_2} \right) \frac{1}{\mu_2 r_2^3} - \frac{\partial V^{\text{eff}}(r_i, \theta_i, \phi_i)}{\partial r_2} \\ \dot{\theta}_2 &= \frac{P_{\theta_2}}{\mu_2 r_2^2}, \quad \dot{P}_{\theta_2} = \frac{P_{\phi_2}^2 \cos \theta_2}{\mu_2 \sin^3 \theta_2 r_2^2} - \frac{\partial V^{\text{eff}}(r_i, \theta_i, \phi_i)}{\partial \theta_2} \\ \dot{\phi}_2 &= \frac{P_{\phi_2}}{\mu_2 \sin^2 \theta_2 r_2^2}, \quad \dot{P}_{\phi_2} = \frac{\partial V^{\text{eff}}(r_i, \theta_i, \phi_i)}{\partial \phi_2}, \end{aligned} \quad (11)$$

of ψ were integrated, for each randomly chosen impact parameter, b , set of orientation angles, θ_i and ϕ_i , and initial center of mass energy, using a fourth-order predictor corrector method. Angles θ_1 and ϕ_1 were chosen in the range $0 \leq \theta_1 \leq \pi$ and $0 \leq \phi_1 \leq 2\pi$, respectively. The initial position of the atom A was chosen to lie along the z axis at an initial distance r_2 sufficiently large in order for the interaction potential to be negligible. In those cases for which the collision is primarily dissociative or reactive the calculation was terminated when the norm of the wave function remaining on the grid was negligible. Otherwise the trajectory was terminated when the distance between the atom and the center of mass of the molecule is larger than $\mathbf{r}_{2\text{max}}$, where we chose $\mathbf{r}_{2\text{max}} = 8 \text{ \AA}$.

Due to the lack of accurate *ab initio* potential energy surfaces for the system N+N₂, we used a London–Eyring–Polanyi–Sato potential energy surface, calculated by Laganá *et al.*⁹ This is likely accurate in describing the three-body affects at long range but is probably not very accurate for close collisions between atoms, as discussed later.

The simultaneous evaluation of the quantal and classical degrees of freedom is performed in the following way. After

setting the initial conditions, the wave function is propagated through a time step $0.5 \Delta t$. This is followed by integrating the classical equations of motion through a time step Δt using the wave function calculated halfway through the time interval. The wave function is then propagated through a full time step using the classical variables calculated at time Δt . This sequence is repeated for the rest of the calculation.

C. Transition probabilities and cross sections

The probability of dissociation is calculated by first projecting the final wave function onto each asymptotic vibrational state to obtain the vibrational transition probabilities, i.e.,

$$P_{v \rightarrow v'} = \left| \int \psi(r_1, t = \infty) \phi_{v'}(r_1) dr_1 \right|^2, \quad (12)$$

where $\phi_{v'}(r_1)$ is the Morse oscillator wave function for vibrational state v' . If a sufficient number of vibrational states are included, then the probability of the collision being non-dissociative and nonreactive, P^{NDR} , is obtained by adding together all the vibrational transition probabilities,

$$P^{\text{NDR}} = \sum_{v'=0}^{v_{\text{max}}} P_{v \rightarrow v'}, \quad (13)$$

where v_{max} is the maximum vibrational state. To determine if a reaction has taken place (i.e., $A+BC \rightarrow AB+C$ or $A+BC \rightarrow AC+B$) we calculate the kinetic energy and the potential energy both between atoms A and C and between atoms A and B. If the kinetic energy plus the potential energy is less than zero for either case, then a reaction has taken place. Due to the presence of the absorbing potential we place a limit on the maximum separation of the BC molecule, $r_{1\text{max}}$. Therefore when $r_1 > r_{1\text{max}}$, the calculation ends. We chose $r_{1\text{max}} = 8 \text{ \AA}$ which is large enough to make a good estimate of the final positions and total energies between all three atoms but is small enough to provide accurate results for the number of grid points used in the FFT calculation. For a given orientation and impact parameter, P^R is either 1 or 0, whereas P^{NDR} can range anywhere between 0 and 1. Therefore we estimate the probability of dissociation, P^D , as follows; if $P^R = 1$ we set $P^D = 0$, otherwise

$$P^D = 1 - P^{\text{NDR}}. \quad (14)$$

This method ensures that P^D is never less than zero. The total integrated cross section for dissociation is obtained by

$$\sigma_D = \int_0^{b_{\text{max}}} b \bar{P}_D db, \quad (15)$$

where b_{max} is the maximum value of the impact parameter b and \bar{P}_D is the probability of dissociation averaged over initial orientation. For a more detailed analysis of the system we calculate also the doubly differential cross section, which is given by

$$\frac{d^2\sigma}{d\Omega d\epsilon} = 2\pi \sum_i^N \frac{P_i(\epsilon, \chi) b_i \Delta b}{2\pi \sin \chi \Delta \chi \Delta \epsilon}, \quad (16)$$

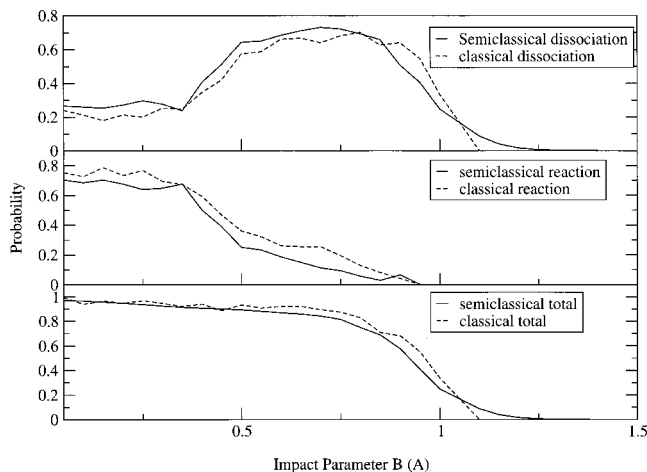


FIG. 1. Top: Probability of dissociation vs impact parameter b in \AA using semiclassical (solid) and classical (dashed) methods for the LEPS PES. Middle: Probability of reaction vs impact parameter b in \AA using semiclassical (solid) and classical (dashed) methods for the LEPS PES. Bottom: Total probability of dissociation and reaction vs impact parameter b in \AA calculated semiclassically (solid) and classically (dashed) using the LEPS PES.

where $P_i(\epsilon, \chi)$ is the probability of the scattering angle being in the range $(\chi - \Delta\chi/2, \chi + \Delta\chi/2)$ with final energy in the range $(\epsilon - \Delta\epsilon/2, \epsilon + \Delta\epsilon/2)$. This is averaged over the number of initial orientations for a given impact parameter b_i . Here N is the total number of impact parameters and ϵ is the energy in the center of mass of the atom-molecule system. For this set of collision partners the net energy transfer from the incident N to the molecule is $T = 1.5[\epsilon_0 - \epsilon]$, where ϵ_0 is the initial energy in the center of mass.

III. RESULTS AND DISCUSSION

Since the dissociation threshold energy of N_2 is 9.91 eV, the dissociation cross sections were calculated at energies, ϵ_0 , between 9 and 40 eV for the ground vibrational state $v = 0$. The wave function was propagated on a grid of 1024 discrete points and the maximum value of the N_2 separation was 8.0 \AA and the minimum value 0.3 \AA . Larger and smaller values for the grid length and the maximum r_2 were tested to find the best values. The maximum vibrational quantum number was calculated using the semiclassical approximation,¹⁰

$$\left(v + \frac{1}{2}\right)^2 = \frac{2\mu_1 D_e}{\hbar^2 \beta^2}, \quad (17)$$

where $D_e = 9.91 \text{ eV}$ is the dissociation energy and $\beta = 2.689/\text{\AA}$, and was found to be $v_{\text{max}} = 67$. For the total dissociation cross sections the maximum value for the impact parameter was taken to be 1.5 \AA and for the differential cross sections was chosen to be 4.0 \AA . For each impact parameter we integrated trajectories for 100 random initial orientations for each energy and we chose $\Delta b = 0.05 \text{ \AA}$. For the absorbing potential we chose $V_0 = 100 \text{ eV}$ and $r_{\text{abs}} = 1.0 \text{ \AA}$.

In Fig. 1 we compare how the probability of dissociation and reaction vary with impact parameter b for the semiclassical and classical calculation using the LEPS PES at the center of mass energy 30 eV. Using the LEPS PES at small

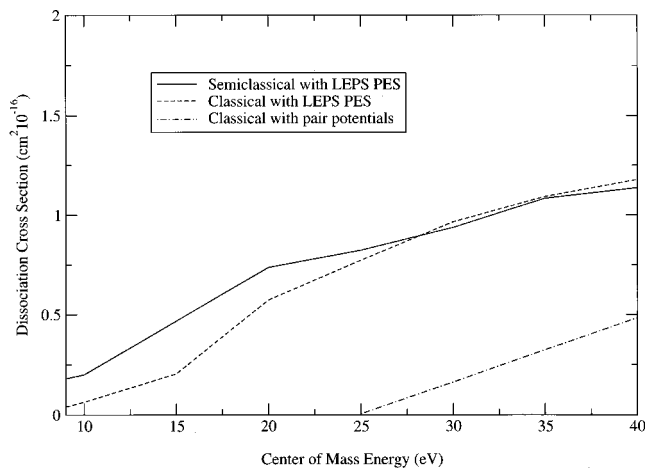


FIG. 2. Integrated dissociation cross sections vs center of mass energy E (eV) ranging from 9 to 40 eV for the semiclassical (solid) and classical (dashed) calculations using the LEPS PES. Also shown is the dissociation cross section calculated classically using the repulsive pair potentials (dot dashed).

impact parameters ($<0.5 \text{ \AA}$) the probability of reaction dominates over that of dissociation but as the impact parameter increases so too does the probability of dissociation until the peak at about 1 \AA .

Collisional dissociation cross sections are shown in Fig. 2 for center of mass energy varying between 9 and 40 eV. These are carried out using the semiclassical method described above and a classical molecular dynamics calculation both using the LEPS PES potential. Also shown in this plot is the classical calculation using the pair potentials obtained by Johnson *et al.*² For energies greater than 20 eV it can be seen that the classical and semiclassical results agree well for the LEPS PES. However, on approaching the dissociation threshold energy (9–20 eV) the semiclassical approximation predicts more dissociation than the classical. The pair potentials are in the form of a repulsive power law potential, given by

$$V_n = \frac{C_n}{r^n}, \quad (18)$$

where r is the separation of the atoms and C_n and n are obtained from data extracted from dissociation cross sections for O+N₂.² The differences between the results of the LEPS PES and those of the power law potentials are primarily due to the three-body terms present in the LEPS PES. That is, as the incident N approaches, the molecule becomes highly distorted. Because the cross section is very sensitive to the details of the potentials in this energy range, accurate potentials are needed.

Finally, in Fig. 3 the semiclassical doubly differential cross sections are given for a range of final energies plotted against the center of mass scattering angle χ .

IV. CONCLUSIONS

We have calculated the dissociation cross sections, the reaction cross sections, and the doubly differential cross sections for N+N₂ for energies in the center of mass of the N

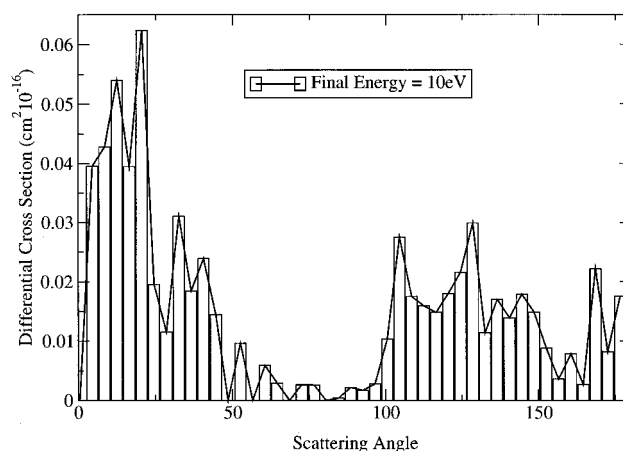
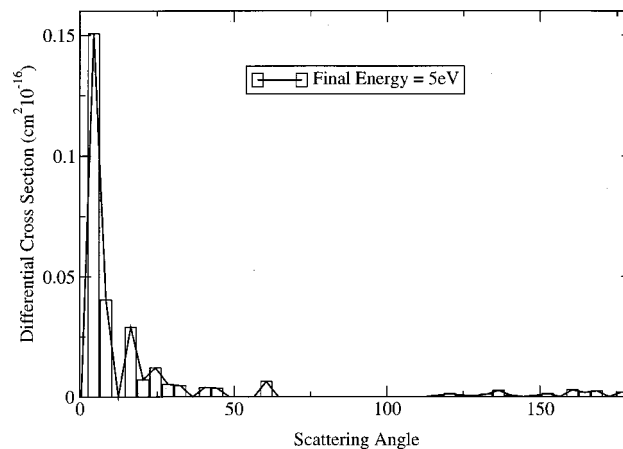


FIG. 3. Doubly differential cross sections plotted against scattering angle χ for the final center of mass energy $\epsilon = 5 \text{ eV}$ (top) and $\epsilon = 10 \text{ eV}$ (bottom), where the initial center of mass energy is 20 eV.

+N₂ system, ϵ_0 , in the range 9–40 eV using a semiclassical method. Because a goal was to better describe the dissociation probability near the threshold region, we used a three-body model potential that can roughly describe the ground state of N₃. This differs considerably from the pair potentials used earlier. For comparison to our semiclassical calculations we also carried out fully classical calculations using the three-body potential.

We find that in the region studied the pair potentials fail dramatically both in describing the dissociation probability with impact parameter and the total dissociation cross sections. However, using the three-body potential constructed from Morse potentials fails at large energy transfers. Therefore, in the region where the repulsive part of the potential dominates ($> \sim 40 \text{ eV}$), an appropriate description of the repulsive part of the potential is needed. In this velocity region, excitations within the ground state multiplet should also be included.

Although our goal was to study collisional dissociation in Titan's upper atmosphere, we found surprisingly large reaction probabilities for the N+N₂ system. However, our cross sections for reaction plus dissociation channels are the most reliable. The separation into reaction and dissociation

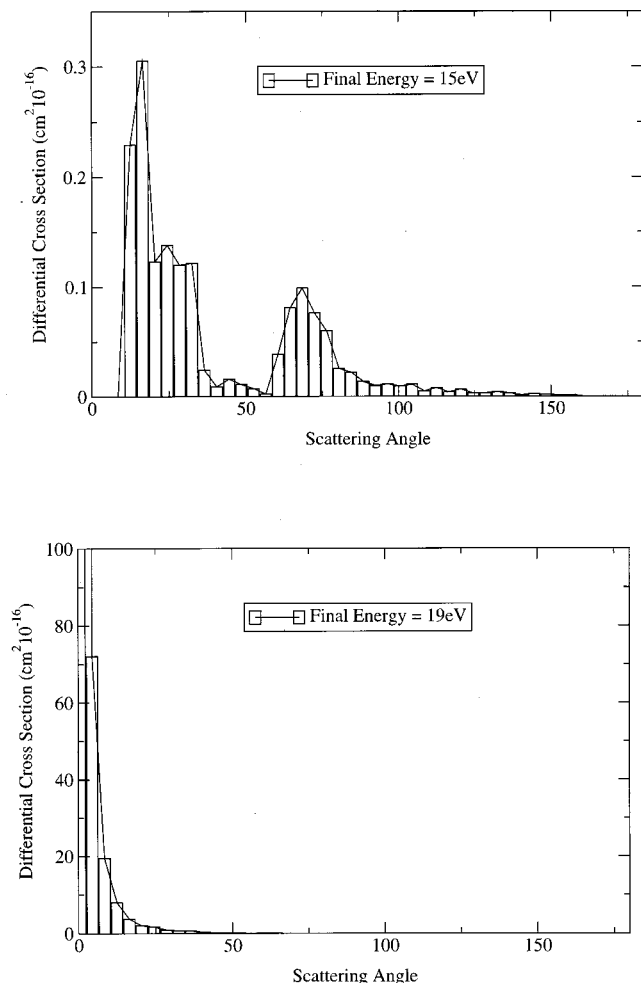


FIG. 4. The same as Fig. 3, but for final center of mass energy $\epsilon = 15$ eV (top) and $\epsilon = 19$ eV (bottom).

cross sections requires that we estimate the position of the dissociated atoms with respect to the incident N. It should also be noted that since a finite grid is used it is difficult to accurately calculate the highly excited vibrational eigenstates up to the dissociation limit. Another method would be to calculate the flux and integrate it to obtain the probability that the molecule has dissociated. It is seen that for both the dissociation and the reaction cross sections, there is rough agreement of the classical result with the semiclassical calculation. Because the semiclassical method allows dissociation when the *average* vibrational state is below the dissociation limit, the semiclassical dissociation cross section is larger than the classical result at the lowest energies as expected. In treating low-energy collisions, the most important improvements that can be made are the use of a better potential surface that accurately treats both the binding and the repulsive regions and, where reactions are important, a fully quantal calculation. The cross sections calculated here are now being incorporated in a particle transport code¹ to describe the heating and loss of Titan's upper atmosphere in preparation for the arrival of the Cassini spacecraft at Saturn (see Fig. 4).

ACKNOWLEDGMENT

This work was supported by the NASA Planetary Atmospheres Program.

APPENDIX: THE SPLIT OPERATOR FAST FOURIER TRANSFORM METHOD

The time propagation of the wave function $\psi(r_1, t)$ is carried out using the symmetrized split operator fast Fourier transform method proposed by Fleck *et al.*¹¹ The following is based on the description by Feit *et al.*¹²

If at time $t = t_0$ the initial wave function $\psi(r, t_0)$ is known on the grid $r = [r_{\min}, r_{\max}]$, where r_{\min} is the minimum value of r and r_{\max} is the maximum, then the solution of the wave function having advanced through a time step Δt is given by

$$\psi(r, t_0 + \Delta t) = \exp\left[-i\left(\frac{-\hbar^2}{2\mu} \frac{\partial}{\partial r^2} + V(r)\right) \frac{\Delta t}{\hbar}\right] \psi(r, t_0). \quad (\text{A1})$$

If Δt is sufficiently small then this can be approximated by

$$\begin{aligned} \psi(r, t_0 + \Delta t) &= \exp\left(-i \frac{\hbar \Delta t}{4\mu} \frac{\partial^2}{\partial r^2}\right) \exp\left(-i \frac{\Delta t}{\hbar} V(r)\right) \\ &\times \exp\left(-i \frac{\hbar \Delta t}{4\mu} \frac{\partial^2}{\partial r^2}\right) \psi(r, t_0), \end{aligned} \quad (\text{A2})$$

which is the symmetrized split operator form.

The solution to the first term in Eq. (A2),

$$\exp\left(-i \frac{\hbar \Delta t}{4\mu} \frac{\partial^2}{\partial r^2}\right),$$

is obtained by using the band-limited Fourier series representation,

$$\begin{aligned} \exp\left(-i \frac{\hbar \Delta t}{4\mu} \frac{\partial^2}{\partial r^2}\right) \psi(r, t_0) \\ = \sum_{n=-N/2+1}^{N/2} \psi_n(t_0 + \Delta t) e^{2\pi i n j / N}, \end{aligned} \quad (\text{A3})$$

where

$$\begin{aligned} \psi_n(t_0 + \Delta t) &= \left(\frac{1}{N} \sum_{j=0}^{N-1} \psi(r_{\min} + \Delta r j, t_0) e^{-2\pi i n j / N}\right) \\ &\times \exp\left[\frac{-i \hbar \Delta t}{4\mu} \left(\frac{2\pi n}{L_0}\right)^2\right]. \end{aligned} \quad (\text{A4})$$

In Eq. (A4), L_0 is the length of the grid $[r_{\min}, r_{\max}]$, N is the number of grid points, and $\Delta r = L_0/N$. The efficiency of this procedure can be increased by using a fast Fourier transform algorithm in evaluation of Eqs. (A3) and (A4). Accurate results are obtained by choosing L_0 large enough so that the amplitude of the wave function is negligible at the grid ends and by choosing Δr small enough to accommodate the spatial bandwidth of the wave function. The time step Δt must also satisfy the condition

$$\Delta t < \hbar / \Delta V_{\max}, \quad (\text{A5})$$

where ΔV_{\max} is the difference between the highest and lowest potential values in the Franck–Condon region.

- ¹V. I. Shematovich, C. Tully, and R. E. Johnson, "Hot nitrogen corona at titan," *Adv. Space Res.* **27**, 1875 (2001).
- ²R. E. Johnson, M. Lui, and C. Tully, "Collisional dissociation cross section for O+O₂, CO and N₂ and N+N₂," *Planet. Space Sci.* (in press).
- ³G. J. Smith, R. S. Gao, B. G. Lindsay, K. A. Smith, and R. F. Stebbings, "Absolute differential cross sections for the scattering of kilo-electron-volt O atoms," *Phys. Rev.* **53**, 1581 (1996).
- ⁴L. Goubert, G. D. Billing, E. Desoppere, and W. Wieme, "Semiclassical calculation of the probabilities for collision-induced vibrational transition in Ar₂," *Chem. Phys. Lett.* **219**, 360 (1994).
- ⁵C. Coletti and G. D. Billing, "Quantum-classical calculation of cross sections and rate constants for the H₂+CN→HCN+H reaction," *J. Chem. Phys.* **113**, 11101 (2000).
- ⁶N. Balakrishnan and G. D. Billing, "Quantum mechanical and semiclassical studies of N+N₂ collisions and their application to thermalization of fast N atoms," *J. Chem. Phys.* **104**, 4005 (1996).
- ⁷H. Kono and S. H. Lin, "Resonance Raman overtone intensity calculations of a matrix-isolated I₂ molecule by the symmetrized split operator fast Fourier transform method," *J. Chem. Phys.* **84**, 1071 (1986).
- ⁸N. Balakrishnan, C. Kalyaaraman, and N. Sathyamurthy, "Time-dependent quantum mechanical approach to reactive scattering and related processes," *Phys. Rep.* **280**, 79 (1997).
- ⁹A. Laganá and E. García, "Temperature dependence of N+N₂ rate coefficients," *J. Phys. Chem.* **98**, 502 (1994).
- ¹⁰M. Carvajal, J. M. A. Rias, and J. Gómez-Camacho, "Configuration localised Morse wavefunctions: Application to vibrational transitions in anharmonic diatomic molecules," *Phys. Rev. A* **59**, 1852 (1999).
- ¹¹J. A. Fleck, Jr., J. R. Morris, and M. D. Feit, "Time dependent propagation of high-energy laser-beams through atmosphere," *Appl. Phys.* **10**, 129 (1976).
- ¹²M. D. Feit, J. A. Fleck, Jr., and A. Steiger, "Solution of the Schrödinger equation by a spectral method," *J. Comput. Phys.* **47**, 412 (1982).